THE PENNSYLVANIA STATE UNIVERSITY
SCHREYER HONORS COLLEGE

DEPARTMENT OF PHYSICS

TIGHT-BINDING ELECTRON TRANSPORT IN REGIONS WITH DISORDER AND THE DIRAC-SEPARATED INFINITE SQUARE WELL

STEPHEN J. THORNTON
SPRING 2019

A thesis
submitted in partial fulfillment
of the requirements
for baccalaureate degrees
in Physics, Astronomy & Astrophysics, and Mathematics
with honors in Physics

Reviewed and approved* by the following:

Jorge O. Sofo
Professor of Physics
Professor of Materials Science and Engineering
Thesis Supervisor

Richard W. Robinett
Professor of Physics
Associate Head for Undergraduate and Graduate Students
Honors Adviser

*Signatures are on file in the Schreyer Honors College.

Abstract

Electron transport in one-dimensional systems can be an analytically tractable and immensely important field of study. To first-order approximation, for instance, carbon nanotubes can be modeled as one-dimensional chains of atomic sites on which an electron can reside. I have considered electron transport in one-dimensional systems under the tight-binding model, where only nearest-neighbor "hopping" of electrons between sites in a discrete chain are considered. In an infinite, homogeneous, perfect chain, the eigenstates are leftward and rightward traveling plane waves that represent electron transport through the chain. Much like in the continuous case, transmission and reflection coefficients can be calculated when these plane wave states are incident on a potential step. Resonances occur when there are interactions between the wave number and the width of the step (just as in the continuous case). A more challenging problem (that can be solved computationally) is to introduce randomly distributed disorder in the region of the step, and calculate the transmission and reflection coefficients for these types of systems. We solve the problem of the transmission and reflection coefficient of this disordered region numerically. I have written code in Mathematica to calculate the transmission and reflection coefficients as a function of incident electron energy given the width of the step and the magnitude of some normally distributed disorder. I find that for slightly disordered systems, the transmission resonances are maintained, but as the disorder increases in magnitude, the transmission probability falls to 0 regardless of the incoming electron energy.

Going to a more continuum-based model, a simple toy model for an electronic state in contact with a large reservoir could be important for understanding leakage of states in quantum computers. The problem is also mathematically interesting, with a measure-valued Hamiltonian governing the time evolution of states. I calculate the probability of finding an electron in some initial state of an infinite square well separated from a larger infinite square well by a Dirac potential as a function of time, and find that the initially confined states leak into the larger reservoir well.

Finally, I go back to the tight binding model and look at a discrete analogue of the continuous system studied above: two finite chains with the degree of separation of the two chains given by a hopping parameter t_1. The eigenstates of the system are exactly solvable (they amount to diagonalizing a finite matrix) and the decoupling is apparent when $t_1 = 0$. The time evolution of these systems can also be easily (numerically) studied. Like the continuous case, the states leak from the initial left well into the right well, and the timescale of leakage varies inversely with the magnitude of the hopping integral between the chains.

Table of Contents

List of Figures

Acknowledgements

I would like to thank my thesis advisor, Prof. Jorge Sofo, for his endless creativity and suggestions for avenues of deeper study. I owe most of my understanding of Bloch theory and undergraduate-level solid state to our weekly meetings.

Chapter 1

1D Electron Transport in Regions with Disorder

1.1 Introduction and Problem Setup

Electron dynamics in 1D systems can be investigated exactly for homogeneous chains. One simple Hamiltonian that describes the dynamics of electrons in such chains is the tight binding Hamiltonian, which is of the form

$$\hat{H} = \sum_i \varepsilon_i \left|i\right\rangle \left\langle i\right| - t_i \left(\left|i\right\rangle \left\langle i+1\right| + \left|i+1\right\rangle \left\langle i\right|\right),$$

with the first term representing the self-energies (ε_i) of each site on which we may find an electron in the chain, the second and third terms represent "hopping" of the electrons leftward and rightward, and t_i representing the "hopping integral", characterizing the probability of jumping between sites. This is an approximation that neglects electron interaction with sites further than nearest-neighbor. For an infinite homogeneous chain, it is well-known that the chain can support (discretized) plane-wave-like states. The electron in free space also has a plane-wave solution, and a commonly studied introductory quantum mechanics problem is to calculate the transmission and reflection coefficients (as functions of energy) of such a plane wave state incident on a potential step with finite width. The same analysis can be done with the discrete chain. I have written code in Mathematica to solve the systems of linear equations associated with these coefficients for the discrete case (and general regions of various site energies). I have also included in my code the ability to repeat regions of disorder and to add normally distributed noise to the site energies. For example, consider a plane wave state incident on a step of 5 sites. In these calculations I set $\hbar = 1$:

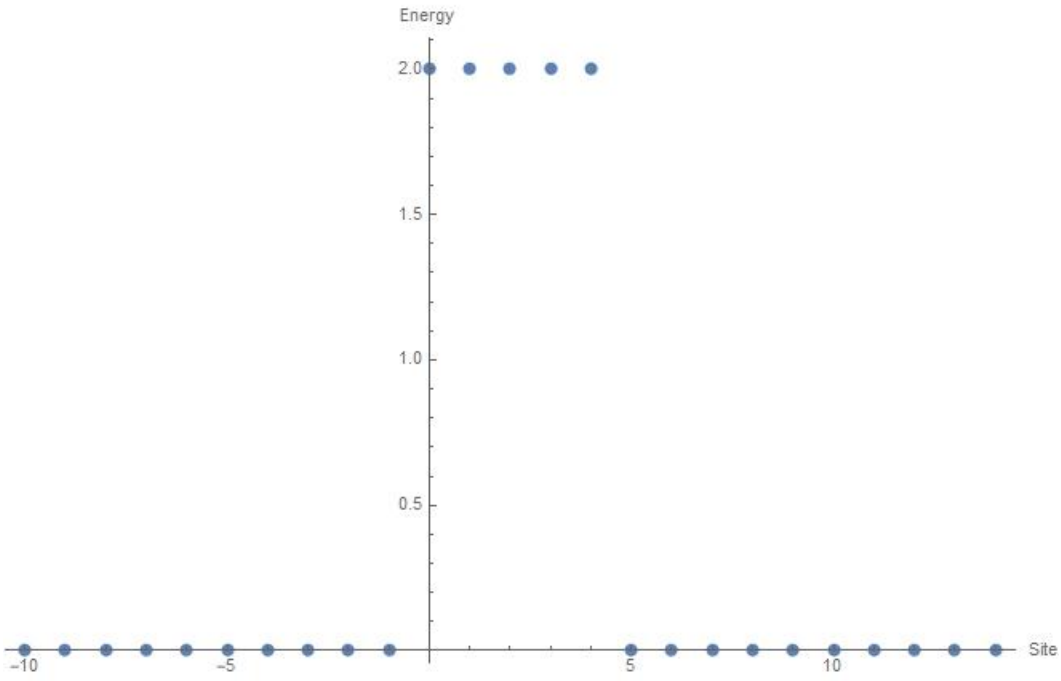

Figure 1.1: The five-site potential step

The transmission and reflection coefficients for electrons with relevant energies are shown below.

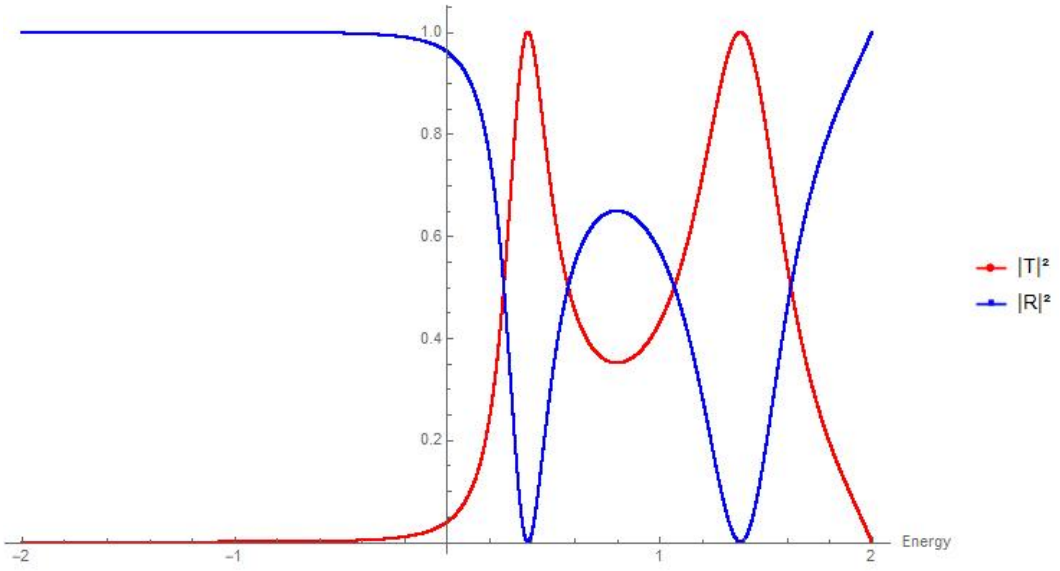

Figure 1.2: Transmission and reflection coefficients for scattering from a five-site step

The behavior of the coefficients are apparently quite complicated, but they agree qualitatively with what is expected from the continuous case. For a step of width L, a standard calculation gives for $E < V$ [1]:

$$|T|^2 = \frac{1}{1 + \frac{1}{4}\frac{V^2}{E(V-E)}\sinh^2\left(L\sqrt{\frac{2m(V-E)}{\hbar^2}}\right)}$$

and for $E > V$:

$$|T|^2 = \frac{1}{1 + \frac{1}{4}\frac{V^2}{E(E-V)}\sin^2\left(L\sqrt{\frac{2m(E-V)}{\hbar^2}}\right)}$$

A plot similar to Figure 1.2 is seen by plotting this coefficient. I plot for $V = 2$ and $L = 5$, again setting $\hbar = 1$:

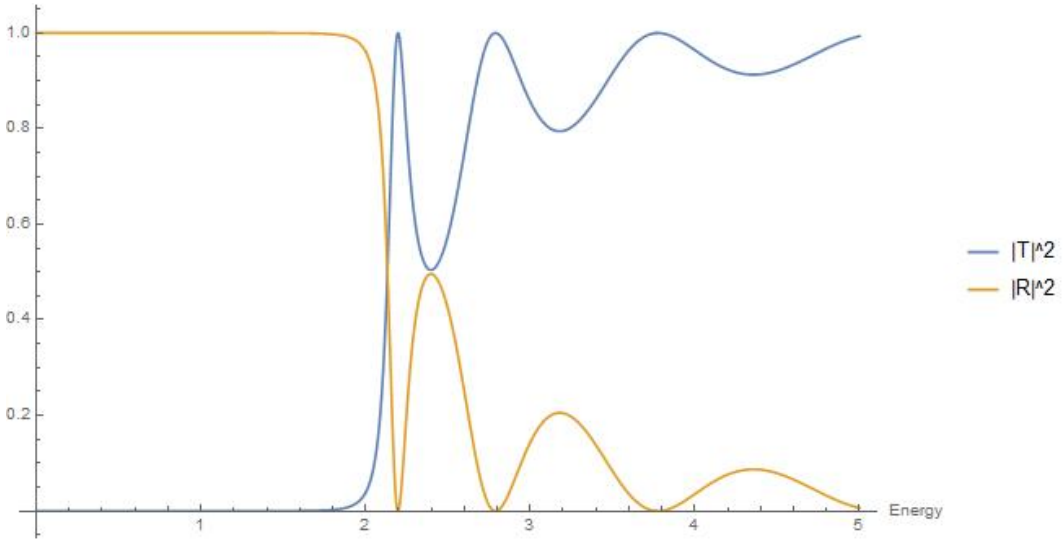

Figure 1.3: Transmission and reflection coefficients for scattering in continuous case

We see similar oscillations in the transmission coefficient, with the peaks representing interference effects where the reflected part of the wave is exactly cancelled. More interestingly, the code for the discrete case allows me to consider steps with disorder. Consider the same step as before, with five sites. I introduce normally distributed disorder at the ten percent level (anything smaller is difficult to notice) and again calculate the transmission and reflection coefficients of the step. The details are shown below.

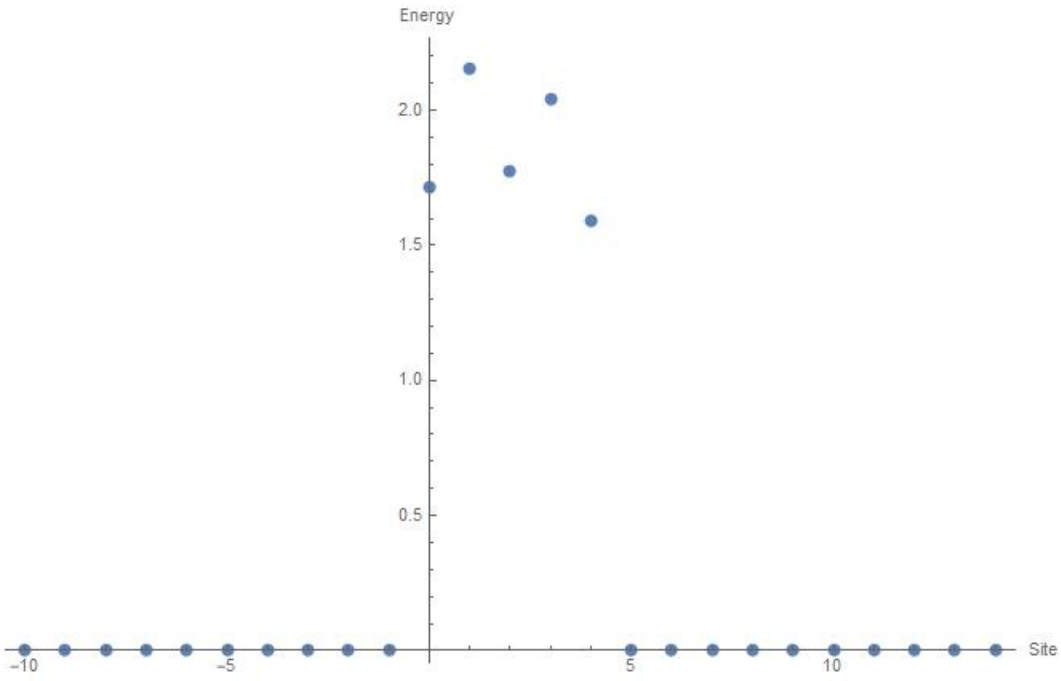

Figure 1.4: The potential step with slight disorder

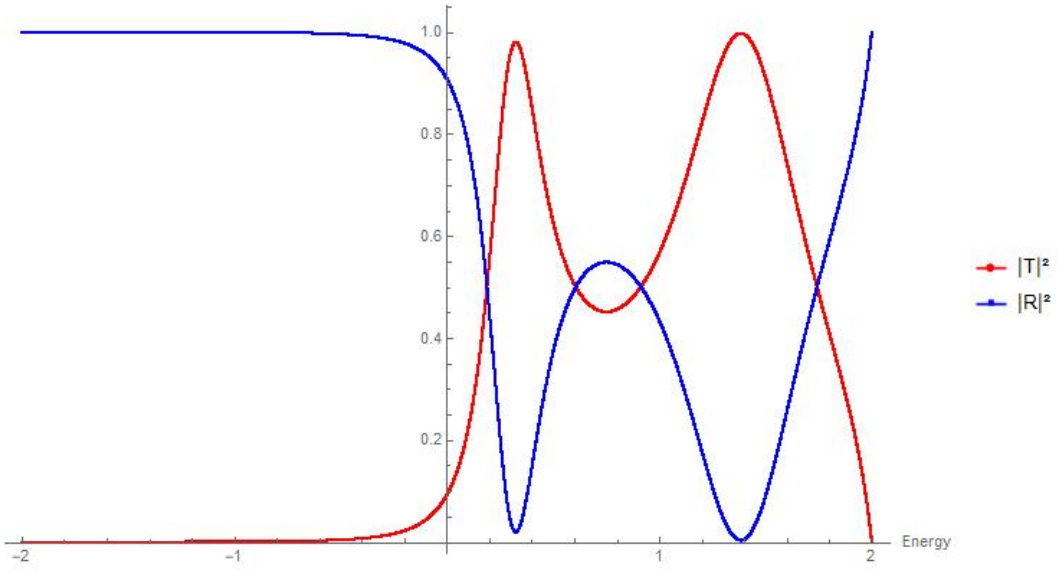

Figure 1.5: Transmission and reflection coefficients for slightly disordered step

Although the plots are qualitatively similar to the step without disorder, I note that the resonances are no longer perfect, i.e., there is a nonzero reflection coefficient even at the local maxima of the transmission coefficient. When the disorder becomes around half of the step energy, the transmission begins to dip significantly, and the plots begin to become very interesting.

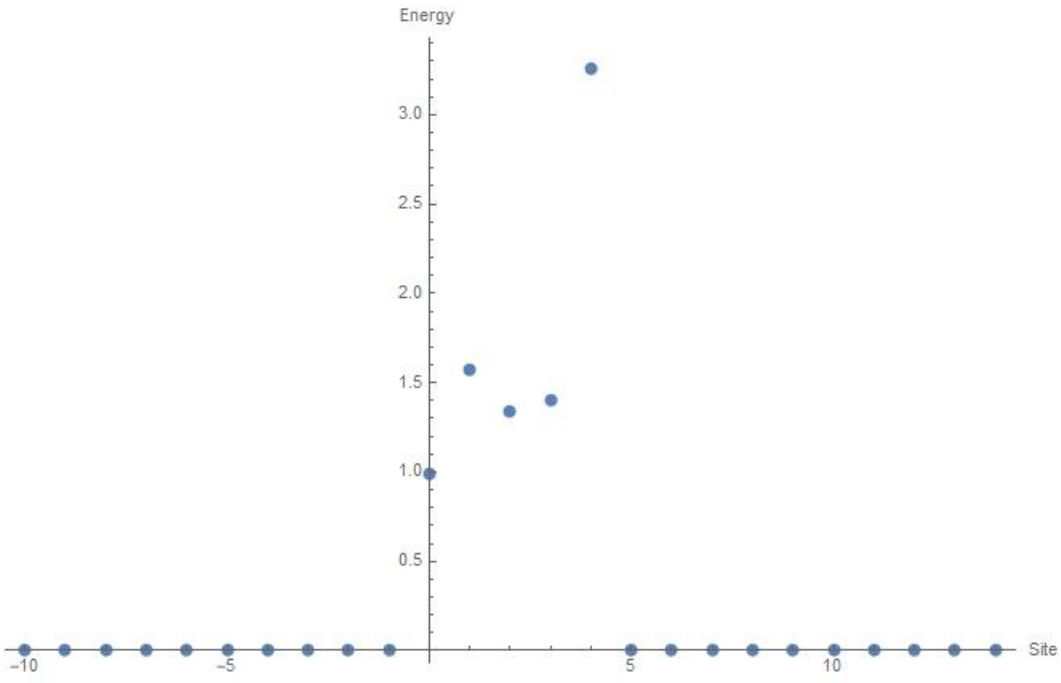

Figure 1.6: The potential step with high disorder

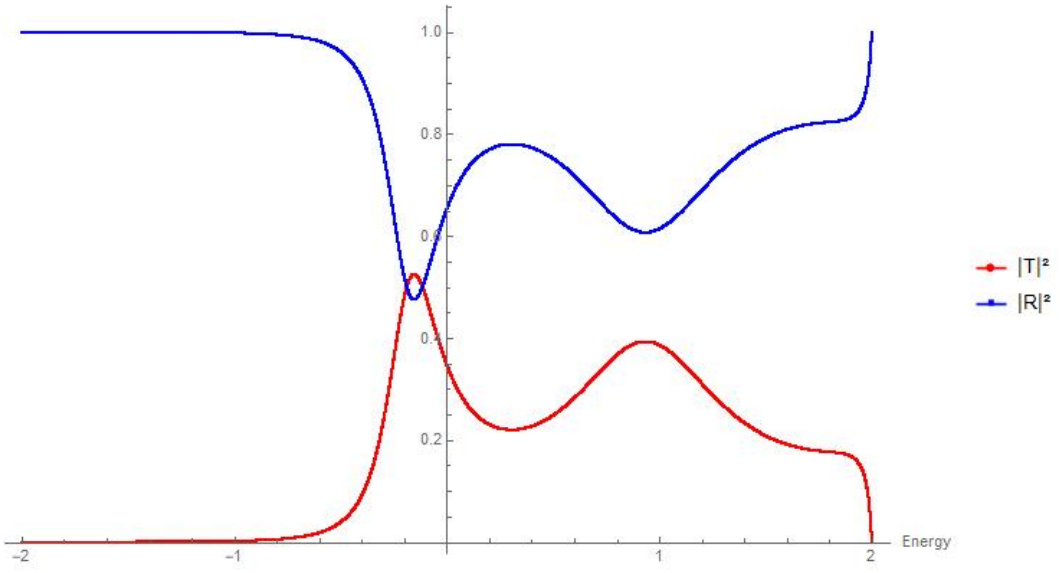

Figure 1.7: Transmission and reflection coefficients for highly disordered step

Although there are still transmission resonances, their locations in electron energy space begin to shift due to the random disorder. Furthermore, the resonances are only reaching around a transmission probability of 1/2, while in the pristine step case, transmission was certain for particular energies. Finally, when the disorder is of order the energy of the step, there is almost no transmission at all. These plots are again shown below.

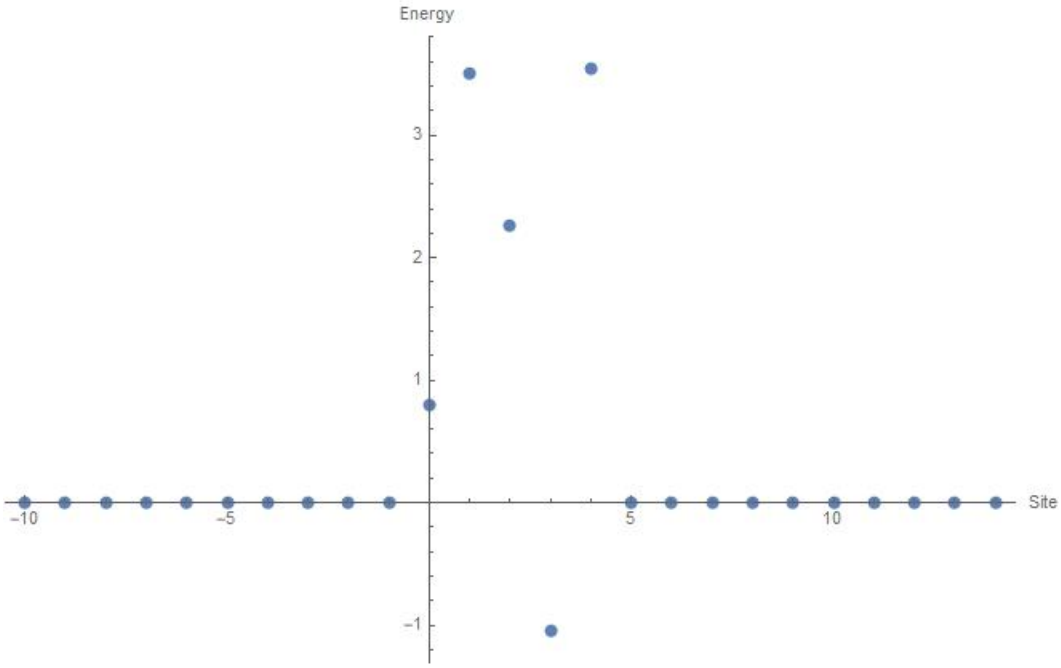

Figure 1.8: The potential step with extreme disorder

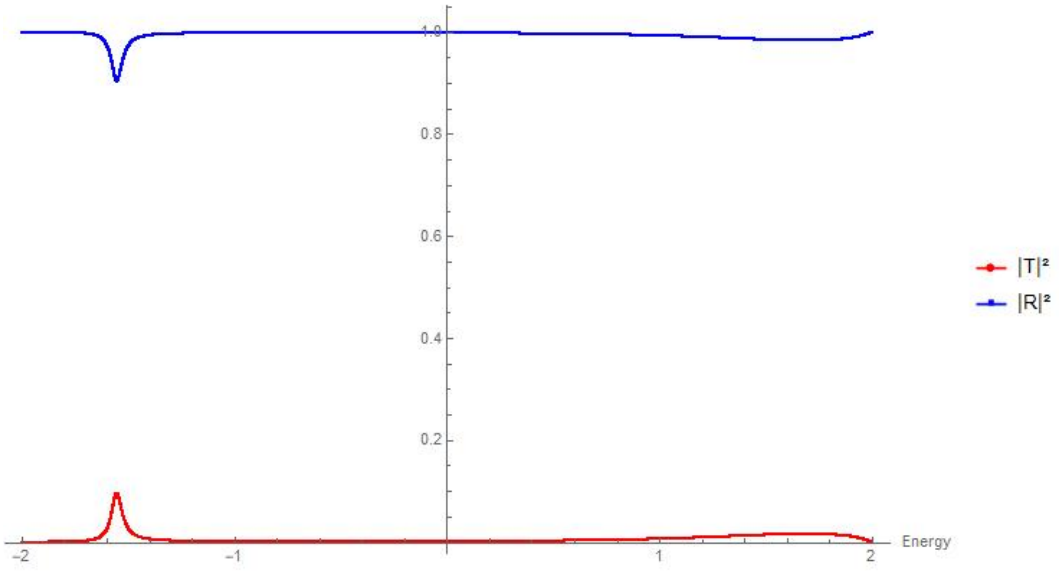

Figure 1.9: Transmission and reflection coefficients for extremely disordered step

The small resonance that appears in the figure above is not special; different random disorders will bring out different fine details in the transmission coefficient plots. This code allows one to vary the number of sites as well. Below is a plot of the ten-site step. The crucial feature that differentiates it from the five-site step is the number of transmission resonances. This is related to the oscillatory behavior of the continuous case: when L is larger, the denominator oscillates faster. One can also think of this as there being more possible "correct k-vectors" to destructively interfere with the reflected wave.

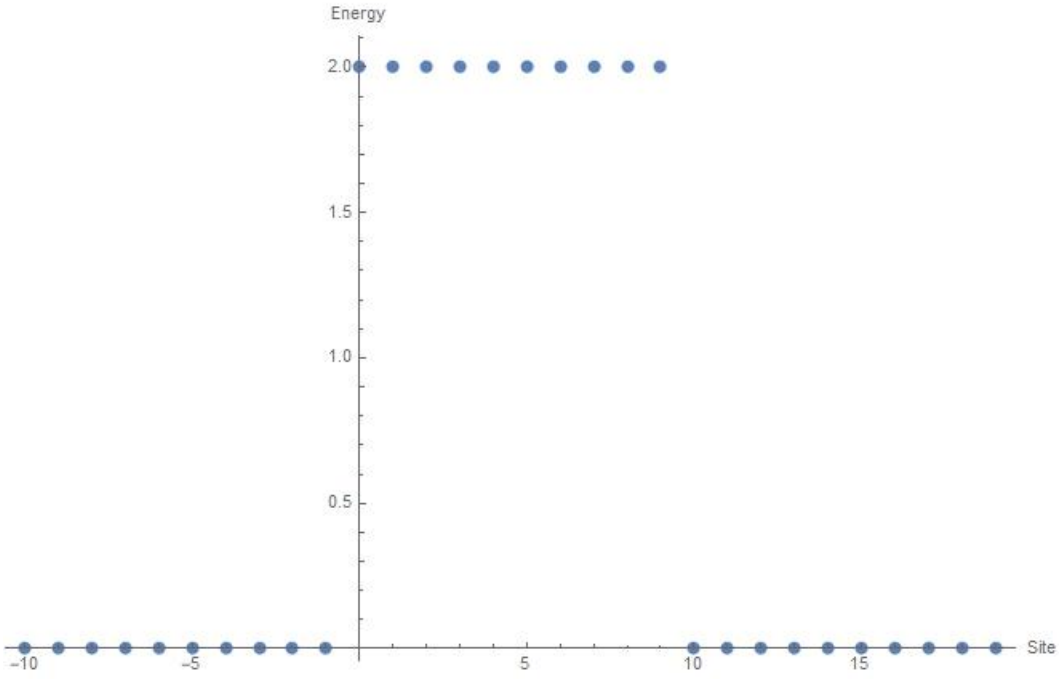

Figure 1.10: The ten-site potential step

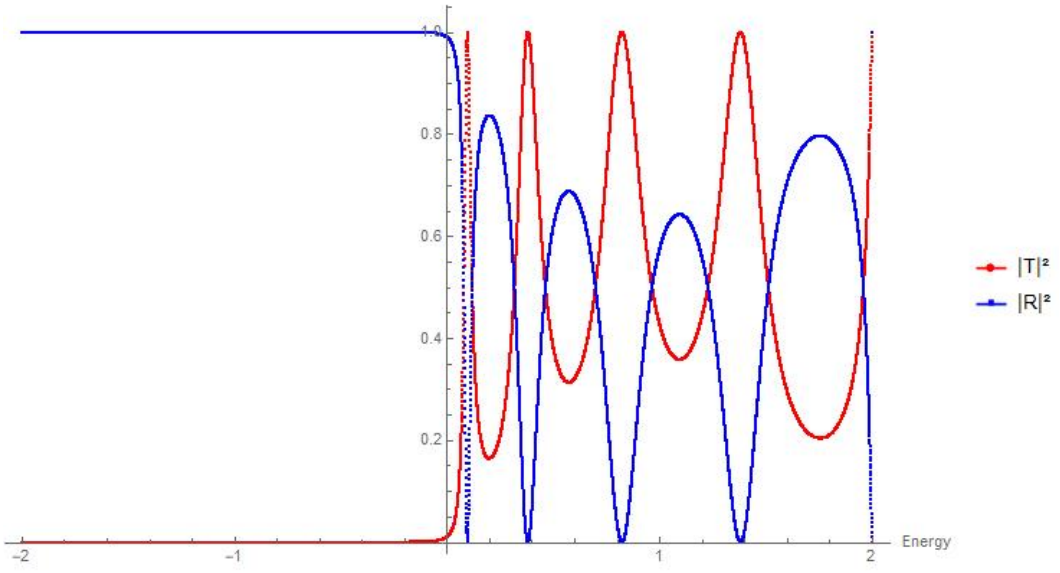

Figure 1.11: Transmission and reflection coefficients for ten-site step

To complete the qualitative analysis of the behavior of these different transmission coefficients for different size steps N, I introduce disorder at the fifty percent level. These plots are shown below.

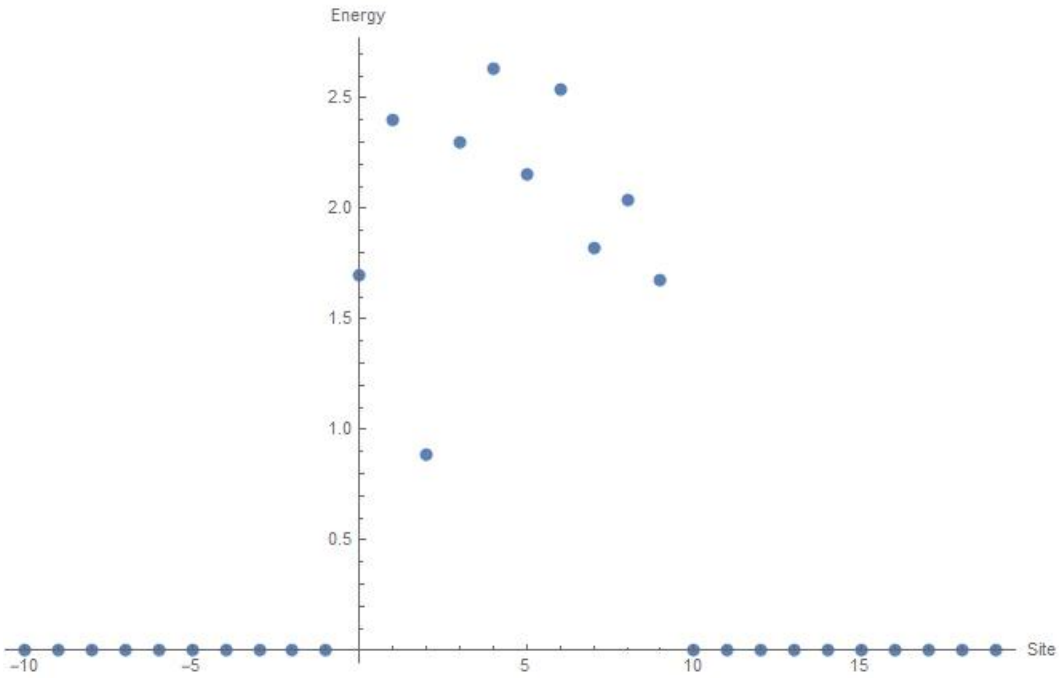

Figure 1.12: The ten-site potential step with disorder

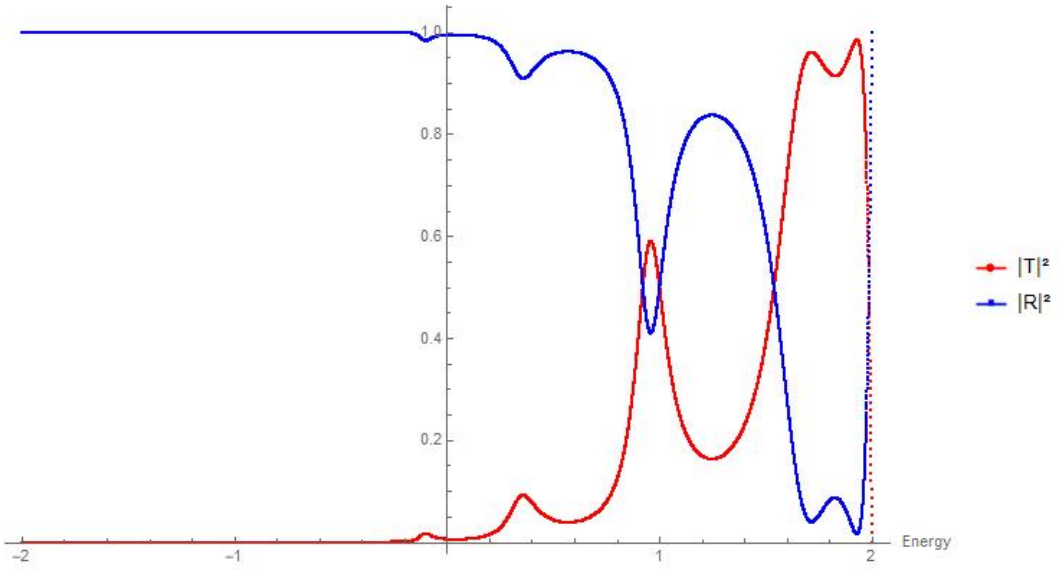

Figure 1.13: Transmission and reflection coefficients for ten-site step with disorder

We again see persistent transmission resonances, but the average transmission drops overall. This code has much more functionality as well, with the ability to repeat regions of disorder. In general, after n repetitions of a disordered site, the transmission decreases as a geometric sequence: $t_n = t_1^n$. This kind of analysis allows for easy determination of resonances.

In this section I studied electron transport in the tight-binding approximation, considering plane-wave electrons with different energies incident on potential steps of varying width. Just as in the continuous case, there appear to be transition resonances associated with interactions between step width and electron k-vector. I also studied how different magnitudes of normally distributed disorder affect the character of the transmission peaks. Many of the peaks remain (though dropping in peak transmission) as the disorder is increased to be half of the size of the step. When the disorder reaches the size of the step itself, there is generally very little transmission.

1.2 Code

Below is the Mathematica code used to generate all of the plots in this section.

```
ClearAll["Global`*"];
mesh = 10000;
eps = 0;
Num = 5;
t = -1;
V = 2;
Disorder = 0.07;
Repetitions = 1;
en = Array[# &, mesh, {-2.0, 2.0}];
diseps = RandomVariate[NormalDistribution[V, Disorder], Num];
(*diseps = {-0.1,0.1};*)
L1 = Range[-10, Num + 9];
L3 = ConstantArray[eps, 10];
L2 = Join[L3, diseps, L3];
SiteEnergies = Transpose@{L1, L2};
L4 = Range[-10, Num*Repetitions + 9];
L5 = diseps;
For[m = 1, m < Repetitions, m++,
  L5 = Join[L5, diseps]];
L6 = Join[L3, L5, L3];
SiteEnergiesRep = Transpose@{L4, L6};
TT = ConstantArray[0, mesh];
RR = ConstantArray[0, mesh];
TTrep = ConstantArray[0, mesh];
RRrep = ConstantArray[0, mesh];
For[i = 1, i < mesh + 1, i++,
 k = ArcCos[(en[[i]] - eps)/(2*t)];
 v1 = {E^(I*k*(Num + 1)), E^(I*k*Num)};
 v2 = {E^(I*k), E^(2*I*k)};
 v3 = {E^(-I*k), E^(-2*I*k)};
 M = {{(en[[i]] - eps)/t, -1}, {1, 0}};
 For[j = 1, j < Num + 1, j++,
  If[j == 1,
   A = {{1, 0}, {0, 1}}];
  Q = {{(en[[i]] - diseps[[j]])/t, -1}, {1, 0}};
  A = Q.A];
 Z = M.A.M;
 A2 = MatrixPower[A, Repetitions];
 Y = M.A2.M;
 v41 = -Z.v2;
 v51 = Z.v3;
 v42 = -Y.v2;
 v52 = Y.v3;
 B = Transpose[{v41, v1}];
 Solns = LinearSolve[B, v51];
```

```
 RR[[i]] = Norm[Solns[[1]]]^2;
 TT[[i]] = Norm[Solns[[2]]]^2;
 J = Transpose[{v42, v1}];
 Solns2 = LinearSolve[J, v52];
 RRrep[[i]] = Norm[Solns2[[1]]]^2;
 TTrep[[i]] = Norm[Solns2[[2]]]^2;]
TransData = Transpose@{en, TT};
RefData = Transpose@{en, RR};
TransRepData = Transpose@{en, TTrep};
RefRepData = Transpose@{en, RRrep};
ListPlot[SiteEnergies, AxesLabel -> {"Site", "Energy"},
 ImageSize -> {600, 600}]
ListPlot[SiteEnergiesRep, AxesLabel -> {"Site", "Energy"},
 ImageSize -> {600, 600}]
ListPlot[{TransData, RefData}, PlotStyle -> {Red, Blue},
 AxesLabel -> {"Energy"},
 PlotLegends ->
  HoldForm@LineLegend[{Red, Blue}, {"|T|\.b2", "|R|\.b2"},
    LegendMarkers -> Automatic], ImageSize -> {600, 600}]
ListPlot[{TransRepData, RefRepData}, PlotStyle -> {Red, Blue},
 AxesLabel -> {"Energy"},
 PlotLegends ->
  HoldForm@LineLegend[{Red, Blue}, {"|T|\.b2", "|R|\.b2"},
    LegendMarkers -> Automatic], ImageSize -> {600, 600}]
```

Chapter 2

Leaky States in a Divided Infinite Square Well: a Wave Function Approach

2.1 Introduction and Problem Setup

I now move into the continuous case. What happens to states in a system that is in contact with a large reservoir? To answer this question, I consider a toy model that evolves as follows: first, a particle is placed into the ground state of an infinite square well with width a. At time $t = 0$, a small linear perturbation is introduced as $V_\varepsilon = \varepsilon x$. This perturbation is turned off at time $t = T$. The particle shifts into a state that is a mixture of the ground state and the first excited state (I assume the mixing with higher-order states is negligible). Next, a large reservoir of width $L - a$ is brought into contact with the right wall of the original square well so that the two are separated by a potential of the form $V_\alpha = \alpha\delta(x - a)$, $\alpha > 0$. What is the probability of finding the particle in the j^{th} state of the original infinite square well at a time t after contact with the reservoir?

2.2 Calculations for an Empty Reservoir

First, I consider the effects of perturbation on the system. I only consider the transition probability from the initial ground state to the first excited state. We have [2]

$$P\left(1 \to 2\right) = P_2 = \left|c_2\right|^2,$$

where

$$c_2 = -\frac{i}{\hbar}\int_0^T dt' \ \exp\left(i\frac{E_2 - E_1}{\hbar}t'\right)V_{21}$$

and

$$V_{21} = \left\langle 2\right| V_\varepsilon \left|1\right\rangle = \frac{2}{a}\varepsilon\int_0^a dx\ x\sin\left(\frac{2\pi x}{a}\right)\sin\left(\frac{\pi x}{a}\right) = -\frac{16a\varepsilon}{9\pi^2}.$$

Hence

$$c_2 = \frac{16a\varepsilon i}{9\pi^2\hbar}\frac{\hbar}{i\left(E_2 - E_1\right)}\left(\exp\left(i\frac{E_2 - E_1}{\hbar}T\right) - 1\right)$$

$$= \frac{16a\varepsilon}{9\pi^2\left(E_2 - E_1\right)}\exp\left(i\frac{E_2 - E_1}{2\hbar}T\right)2i\sin\left(\frac{E_2 - E_1}{2\hbar}T\right)$$

Inserting the expression for the energy states of the infinite square well gives

$$c_2 = \frac{64ma^3\varepsilon}{27\pi^4\hbar^2}\sin\left(\frac{3\pi^2\hbar}{4ma^2}T\right)i\exp\left(i\frac{3\pi^2\hbar}{4ma^2}T\right)$$

and so

$$P_2 = \left|c_2\right|^2 = \frac{4096m^2a^6\varepsilon^2}{729\pi^8\hbar^4}\sin^2\left(\frac{3\pi^2\hbar}{4ma^2}T\right).$$

From now on it will be assumed that the particle is in the state

$$\left|\psi_0\right\rangle = \left(1 - P_2\right)^{\frac{1}{2}}\left|1\right\rangle + P_2^{\frac{1}{2}}\left|2\right\rangle.$$

I'll call this state in its position basis $\psi_0(x)$. Now we bring a reservoir and place it in contact with the original infinite square well so that the two wells are separated by a potential of $V_\alpha = \alpha\delta(x-a)$, $\alpha > 0$. I now find the eigenstates of this system. This amounts to solving

$$-\frac{\hbar^2}{2m}\frac{d^2}{dx^2}\psi(x) + \alpha\delta(x-a)\psi(x) = E\psi(x).$$

This separates into two standard waves of the form

$$\begin{cases} \psi_L(x) = A_r e^{ikx} + A_l e^{-ikx}, & 0 < x < a \\ \psi_R(x) = B_r e^{ikx} + B_l e^{-ikx}, & a < x < L \end{cases} \tag{2.1}$$

where

$$k = \frac{\sqrt{2mE}}{\hbar}.$$

The boundary conditions are as follows:

$$\psi(0) = \psi_L(0) = 0$$

$$\psi(L) = \psi_R(L) = 0$$

$$\psi_L(a) = \psi_R(a)$$

Since the potential is infinite at $x = a$, there will be a discontinuity in the derivative of $\psi(x)$ there. To derive this, I integrate the time independent Schrödinger equation over a small region centered at a:

$$\lim_{\varepsilon\to 0^+}\left[-\frac{\hbar^2}{2m}\int_{a-\varepsilon}^{a+\varepsilon}\frac{d^2}{dx^2}\psi(x)\,dx + \alpha\int_{a-\varepsilon}^{a+\varepsilon}\delta(x-a)\psi(x)\,dx\right] = E\lim_{\varepsilon\to 0^+}\int_{a-\varepsilon}^{a+\varepsilon}\psi(x)\,dx$$

The right hand side tends to 0 since ψ is square-integrable on $[0, L]$. Evaluating the left hand side gives the constraint on discontinuity in the derivative:

$$\psi'_R(a) - \psi'_L(a) = \frac{2m\alpha}{\hbar^2}\psi(a).$$

These constraints can be put together to find admissible values of k. Eliminating the coefficients on the wave functions gives the following (transcendental, unfortunately) equation for k:

$$\cot\left(k\left(L-a\right)\right) + \cot\left(ka\right) = -\frac{2m\alpha}{\hbar^2 k}.$$

Plotting each of these functions shows that for fixed L, a, m, and α, this gives a family of discretized solutions k_n. A plot is shown below in Figure 2.1 of the left hand side and the right hand side as functions of k, with all parameters (including $\hbar$) set to 1 except L, which is set to 10.

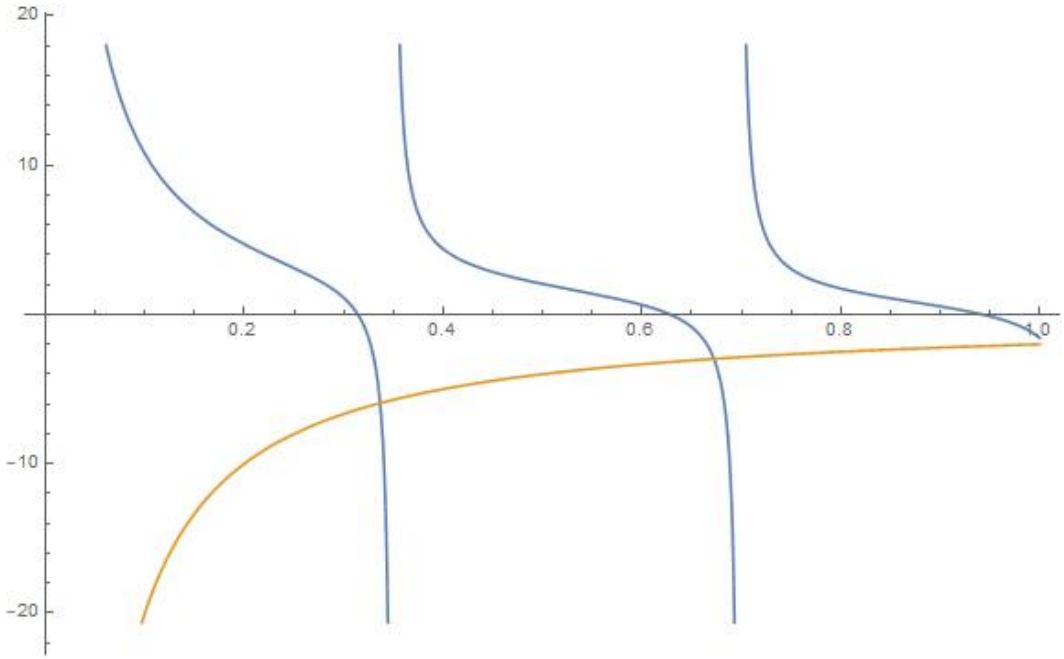

Figure 2.1: Discretized k for separated square well

From now on, I will refer to the n^{th} solution of this equation as k_n. From above, the energies associated with the eigenstates of this potential are

$$E_n = \frac{\hbar^2 k_n^2}{2m}.$$

Lots of algebra gives that the eigenstates are given by

$$\begin{cases} \psi_L^n(x) = A_n \sin(k_n x), & 0 < x < a \\ \psi_R^n(x) = \frac{A_n \sin(k_n a)}{e^{ik_n a} - e^{ik_n(2L-a)}} \left(e^{ik_n x} - e^{ik_n(2L-x)}\right), & a < x < L \end{cases} \tag{2.2}$$

where A_n is fixed by the normalization condition. Even more computation gives:

$$A_n = \left(\frac{4k_n \sin^2\left(k_n\left(L-a\right)\right)}{\sin\left(k_n a\right)\left(2k_n L \sin\left(k_n a\right) + \cos\left(k_n\left(2L-a\right)\right) - \cos\left(k_n a\right)\right)} \right)^{\frac{1}{2}}$$

Call these eigenstates of the new Dirac-separated system ψ_n. Note that A_n is bounded as $n \to \infty$ since the linear k_n terms in the numerator and denominator begin to dominate (this is important when evaluating convergence later). It remains to calculate the probabilities that the particle is found in the ground state and the first excited state of the *original* square well of width a as a function of time. The probability that the particle is found in the j^{th} state of the original oscillator is

$$P_j(t) = |\langle j|\psi(t)\rangle|^2 = \left| \int_0^a dx \, \sqrt{\frac{2}{a}} \sin\left(\frac{j\pi x}{a}\right) \psi\left(x,t\right) \right|^2$$

The function $\psi(x,t)$ is found by expanding the perturbed two-level state in the eigenbasis of the Dirac-separated well $\{\phi_n\}$:

$$\psi(x,t) = \sum_{n=1}^{\infty} \langle \phi_n | \psi_0 \rangle \, \phi_n(x) \exp\left(-i\frac{E_n}{\hbar}t\right) = \sum_{n=1}^{\infty} c_n \phi_n(x) \exp\left(-i\frac{E_n}{\hbar}t\right)$$

Computing the coefficients (keeping in mind $\psi_0(x) \equiv 0$ for $x > a$) gives:

$$c_n = \int_0^L dx \; \phi_n(x)\psi_0(x)$$

$$= A_n \left(1 - P_2\right)^{\frac{1}{2}} \sqrt{\frac{2}{a}} \int_0^a dx \;\; \sin\left(k_n x\right) \sin\left(\frac{\pi x}{a}\right) + A_n P_2^{\frac{1}{2}} \sqrt{\frac{2}{a}} \int_0^a dx \;\; \sin\left(k_n x\right) \sin\left(\frac{2\pi x}{a}\right)$$

$$= A_n \left(1 - P_2\right)^{\frac{1}{2}} \sqrt{\frac{2}{a}} \left(\frac{\pi a \sin(k_n a)}{\pi^2 - a^2 k_n^2}\right) + A_n P_2^{\frac{1}{2}} \sqrt{\frac{2}{a}} \left(\frac{2\pi a \sin(k_n a)}{a^2 k_n^2 - 4\pi^2}\right)$$

Going back to the full expression for the probabilities, inserting the expression for $\psi(x,t)$, and doing some moving around of sums gives

$$P_j(t) = \left| \sum_{n=1}^{\infty} c_n \sqrt{\frac{2}{a}} \exp\left(-i\frac{E_n}{\hbar}t\right) A_n \int_0^a dx \;\; \sin\left(\frac{j\pi x}{a}\right) \sin\left(k_n x\right) \right|^2$$

$$= \left| \sum_{n=1}^{\infty} c_n \sqrt{\frac{2}{a}} \exp\left(-i\frac{E_n}{\hbar}t\right) A_n \left(\frac{(-1)^j j\pi a \sin(k_n a)}{a^2 k_n^2 - \pi^2 j^2}\right) \right|^2$$

$$= 2j^2\pi^2 a \left| \sum_{n=1}^{\infty} A_n c_n \exp\left(-i\frac{E_n}{\hbar}t\right) \frac{\sin(k_n a)}{a^2 k_n^2 - \pi^2 j^2} \right|^2$$

$$= 2j^2\pi^2 a \left| \sum_{n=1}^{\infty} A_n c_n \exp\left(-i\frac{\hbar k_n^2}{2m}t\right) \frac{\sin(k_n a)}{a^2 k_n^2 - \pi^2 j^2} \right|^2$$

Recall that

$$A_n c_n = A_n^2 \left(1 - P_2\right)^{\frac{1}{2}} \sqrt{\frac{2}{a}} \left(\frac{\pi a \sin(k_n a)}{\pi^2 - a^2 k_n^2}\right) + A_n^2 P_2^{\frac{1}{2}} \sqrt{\frac{2}{a}} \left(\frac{2\pi a \sin(k_n a)}{a^2 k_n^2 - 4\pi^2}\right)$$

$$= \frac{4k_n \sin^2\left(k_n\left(L-a\right)\right)}{\sin\left(k_n a\right)\left(2k_n L \sin\left(k_n a\right) + \cos\left(k_n\left(2L-a\right)\right) - \cos\left(k_n a\right)\right)} \times$$

$$\times \left(\left(1 - \frac{4096 m^2 a^6 \varepsilon^2}{729\pi^8\hbar^4} \sin^2\left(\frac{3\pi^2\hbar}{4ma^2}T\right)\right)^{\frac{1}{2}} \sqrt{\frac{2}{a}} \left(\frac{\pi a \sin(k_n a)}{\pi^2 - a^2 k_n^2}\right) + \right.$$

$$\left. + \left(\frac{4096 m^2 a^6 \varepsilon^2}{729\pi^8\hbar^4} \sin^2\left(\frac{3\pi^2\hbar}{4ma^2}T\right)\right)^{\frac{1}{2}} \sqrt{\frac{2}{a}} \left(\frac{2\pi a \sin(k_n a)}{a^2 k_n^2 - 4\pi^2}\right) \right).$$

Hence we have a full (almost) closed form for the result, so I will summarize. Beginning with a particle in the ground state of an infinite square well with width a, a perturbation of the form $V_\varepsilon = \varepsilon x$ is applied for time T, mixing it into all of the excited states. I consider the mixing into states higher than $n = 2$ to be negligible. Next, the particle is brought into contact with a large reservoir of size $L - a$, with $L \gg a$, and the two are separated by a Dirac potential of the form $V_\alpha = \alpha\delta(x - a)$, $\alpha > 0$. After a time t has passed since the original well has touched the reservoir, the probability of finding the particle in the j^{th} state of the original infinite square well is

$$P_j(t) = 64j^2\pi^2 \left| \sum_{n=1}^{\infty} \frac{k_n \sin^2\left(k_n\left(L-a\right)\right)}{\sin\left(k_n a\right)\left(2k_n L\sin\left(k_n a\right) + \cos\left(k_n\left(2L-a\right)\right) - \cos\left(k_n a\right)\right)} \times \right.$$

$$\times \left(\left(1 - \frac{4096m^2a^6\varepsilon^2}{729\pi^8\hbar^4}\sin^2\left(\frac{3\pi^2\hbar}{4ma^2}T\right)\right)^{\frac{1}{2}} \left(\frac{\pi a\sin(k_n a)}{\pi^2 - a^2k_n^2}\right) + \right.$$

$$\left. \left. + \left(\frac{4096m^2a^6\varepsilon^2}{729\pi^8\hbar^4}\sin^2\left(\frac{3\pi^2\hbar}{4ma^2}T\right)\right)^{\frac{1}{2}} \left(\frac{2\pi a\sin(k_n a)}{a^2k_n^2 - 4\pi^2}\right)\right) \exp\left(-i\frac{\hbar k_n^2}{2m}t\right) \frac{\sin(k_n a)}{a^2k_n^2 - \pi^2 j^2} \right|^2$$

where k_n are the solutions to the transcendental equation

$$\cot\left(k\left(L-a\right)\right) + \cot\left(ka\right) = -\frac{2m\alpha}{\hbar^2 k}.$$

It appears terms in the summand go asymptotically as

$$\frac{1}{k_n^4},$$

and the k_n are asymptotically equally spaced, so the sum should rapidly converge. To see that the k_n are asymptotically equally spaced, note that the right hand side of the equation determining k goes to 0 and then the equation becomes

$$\cot\left(k\left(L-a\right)\right) + \cot\left(ka\right) = 0$$

$$\cot\left(k\left(L-a\right)\right) = \cot\left(-ka\right) \implies k_n\left(L-a\right) = -k_n a + n\pi$$

$$k_n = \frac{\pi n}{L}.$$

This is fascinating, because these are the k values for the infinite square well of total width L! This makes intuitive sense, because for very large n the eigenstates are oscillating so rapidly that they do not "see" the delta potential: the derivatives of $\psi_n(x)$ for these large n are huge in magnitude as compared to the discontinuity α introduced by the delta function.

The next step is to calculate these probabilities (computationally) and see if they agree with what we expect for this kind of system. Plotted below in Figure 2.2 are the probabilities of the first four states as a function of time for carefully chosen values of the constants.

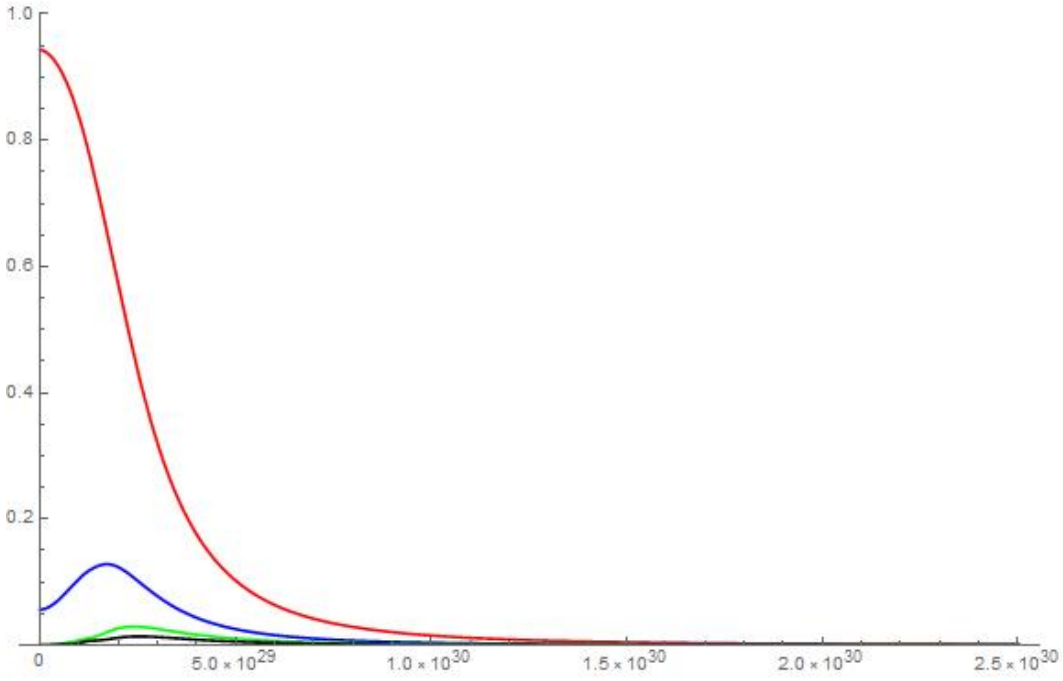

Figure 2.2: First four states leaking into empty reservoir

As expected, after some initial settling, the states leak into the empty reservoir.

2.3 Code

Below is the Mathematica code used to generate the final plot in this section.

```
$MinPrecision = $MaxPrecision = 10000;
numterms = 10000;
hbar = 1.055*10^(-34);
m = 1;
a = 0.01;
L = \[Pi]*E; (*to make sure there are no accidental degeneracies*)
T = ((4*m*a^2)/(3*\[Pi]^2*hbar))*(\[Pi]/
     2);(*to maximize amount in n=2 state*)
alpha = hbar^2/(2*m*L);
eps = 0.1*(hbar^2*\[Pi]^4/(m*
        a^3)); (*to make the perturbation small, but not too small*)
k = ConstantArray[0, numterms];
For[n = 1, n < numterms + 1, n++,
  k[[n]] =
    x /. FindRoot[
      Cot[x*(L - a)] + Cot[x*a] + 2*m*alpha/(hbar^2*x), {x,
       n*\[Pi]/L}];];
P1[t_] :=
```

```
  64*\[Pi]^2 Abs[
     Sum[Abs[(k[[n]]*
           Sin[k[[n]]*(L - a)]^2)/((Sin[
             k[[n]]*a])*(2*k[[n]]*L*Sin[k[[n]]*a] +
             Cos[k[[n]]*(2 L - a)] -
             Cos[k[[n]]*
               a]))]*((1 - (4096*m^2*a^6*eps^2/(729*\[Pi]^8*hbar^4))*
              Sin[3*\[Pi]^2*hbar*T/(4*m*a^2)]^2)^(1/2)*(\[Pi]*a*
            Sin[k[[n]]*a]/(\[Pi]^2 - a^2*k[[n]]^2)) + ((4096*m^2*a^6*
               eps^2/(729*\[Pi]^8*hbar^4))*
             Sin[3*\[Pi]^2*hbar*T/(4*m*a^2)]^2)^(1/2)*(2*\[Pi]*a*
            Sin[k[[n]]*a]/(a^2*k[[n]]^2 - 4 \[Pi]^2)))*
       Exp[-I*hbar*k[[n]]^2*t/(2*m)]*
       Sin[k[[n]]*a]/(a^2 k[[n]]^2 - \[Pi]^2), {n, numterms}]]^2;
P2[t_] :=
  64*4*\[Pi]^2 Abs[
     Sum[Abs[(k[[n]]*
           Sin[k[[n]]*(L - a)]^2)/((Sin[
             k[[n]]*a])*(2*k[[n]]*L*Sin[k[[n]]*a] +
             Cos[k[[n]]*(2 L - a)] -
             Cos[k[[n]]*
               a]))]*((1 - (4096*m^2*a^6*eps^2/(729*\[Pi]^8*hbar^4))*
              Sin[3*\[Pi]^2*hbar*T/(4*m*a^2)]^2)^(1/2)*(\[Pi]*a*
            Sin[k[[n]]*a]/(\[Pi]^2 - a^2*k[[n]]^2)) + ((4096*m^2*a^6*
               eps^2/(729*\[Pi]^8*hbar^4))*
             Sin[3*\[Pi]^2*hbar*T/(4*m*a^2)]^2)^(1/2)*(2*\[Pi]*a*
            Sin[k[[n]]*a]/(a^2*k[[n]]^2 - 4 \[Pi]^2)))*
       Exp[-I*hbar*k[[n]]^2*t/(2*m)]*
       Sin[k[[n]]*a]/(a^2 k[[n]]^2 - 4*\[Pi]^2), {n, numterms}]]^2;
P3[t_] :=
  64*9*\[Pi]^2 Abs[
     Sum[Abs[(k[[n]]*
           Sin[k[[n]]*(L - a)]^2)/((Sin[
             k[[n]]*a])*(2*k[[n]]*L*Sin[k[[n]]*a] +
             Cos[k[[n]]*(2 L - a)] -
             Cos[k[[n]]*
               a]))]*((1 - (4096*m^2*a^6*eps^2/(729*\[Pi]^8*hbar^4))*
              Sin[3*\[Pi]^2*hbar*T/(4*m*a^2)]^2)^(1/2)*(\[Pi]*a*

            Sin[k[[n]]*a]/(\[Pi]^2 - a^2*k[[n]]^2)) + ((4096*m^2*a^6*
               eps^2/(729*\[Pi]^8*hbar^4))*
             Sin[3*\[Pi]^2*hbar*T/(4*m*a^2)]^2)^(1/2)*(2*\[Pi]*a*
            Sin[k[[n]]*a]/(a^2*k[[n]]^2 - 4 \[Pi]^2)))*
       Exp[-I*hbar*k[[n]]^2*t/(2*m)]*
       Sin[k[[n]]*a]/(a^2 k[[n]]^2 - 9*\[Pi]^2), {n, numterms}]]^2;
```

```
P4[t_] :=
  64*16*\[Pi]^2 Abs[
     Sum[Abs[(k[[n]]*
           Sin[k[[n]]*(L - a)]^2)/((Sin[
             k[[n]]*a])*(2*k[[n]]*L*Sin[k[[n]]*a] +
             Cos[k[[n]]*(2 L - a)] -
             Cos[k[[n]]*
               a]))]*((1 - (4096*m^2*a^6*eps^2/(729*\[Pi]^8*hbar^4))*
              Sin[3*\[Pi]^2*hbar*T/(4*m*a^2)]^2)^(1/2)*(\[Pi]*a*
            Sin[k[[n]]*a]/(\[Pi]^2 - a^2*k[[n]]^2)) + ((4096*m^2*a^6*
               eps^2/(729*\[Pi]^8*hbar^4))*
             Sin[3*\[Pi]^2*hbar*T/(4*m*a^2)]^2)^(1/2)*(2*\[Pi]*a*
            Sin[k[[n]]*a]/(a^2*k[[n]]^2 - 4 \[Pi]^2)))*
       Exp[-I*hbar*k[[n]]^2*t/(2*m)]*
       Sin[k[[n]]*a]/(a^2 k[[n]]^2 - 16*\[Pi]^2), {n, numterms}]]^2;
Plot[{P1[t], P2[t], P3[t], P4[t]}, {t, 0, 2.5*10^30},
 ImageSize -> Large, PlotRange -> {0, 1},
 PlotStyle -> {Red, Blue, Green, Black}]
```

Chapter 3

A Discrete Analogue to the Continuous System

3.1 Introduction and Problem Setup

Following the kinds of matrix systems considered in the first chapter, we can consider a tight-binding analogue of the Dirac-separated square well. The Hamiltonian for this discrete system is given by

$$\hat{H} = -\sum_{i=1}^{L-1} t_i \left(|i\rangle \langle i+1| + |i+1\rangle \langle i| \right)$$

with $t_i = t_0$ for $i \neq L_s$ and $t_{L_s} = t_1$. This represents the Hamiltonian for two (finite) homogeneous tight binding chains of lengths L_s and $L - L_s$ with hopping parameter t_0 that are separated by a coupling of strength t_1. The coupling strength t_1 is similar to the parameter α in the continuous case: when $t_1 = 0$, the chains are fully separated from each other, while when $t_1 = t_0$, the two chains together are effectively one single chain. Solving for the dynamics of the system becomes a matrix diagonalization problem (since the chains are both finite). That the chain is decoupled when $t_1 = 0$ can be easily seen from the form of the Hamiltonian matrix in its site position basis:

$$\begin{pmatrix}
0 & t_0 & 0 & 0 & 0 & 0 & 0 & \cdots & 0 \\
t_0 & 0 & t_0 & 0 & 0 & 0 & 0 & \cdots & 0 \\
0 & t_0 & 0 & t_0 & 0 & 0 & 0 & \cdots & 0 \\
0 & 0 & t_0 & 0 & t_0 & 0 & 0 & \cdots & 0 \\
 & & & & \ddots & & & & \\
\cdots & 0 & 0 & t_0 & 0 & t_0 & 0 & 0 & \cdots \\
\cdots & 0 & 0 & 0 & t_0 & 0 & t_1 & 0 & \cdots \\
\cdots & 0 & 0 & 0 & 0 & t_1 & 0 & t_0 & \cdots \\
\cdots & 0 & 0 & 0 & 0 & 0 & t_0 & 0 & \cdots \\
 & & & & \ddots & & & & \\
\cdots & 0 & 0 & 0 & 0 & 0 & 0 & t_0 & 0
\end{pmatrix}$$

When the coupling constants t_1 are 0, the row reduction algorithm that diagonalizes this Hermitian matrix can be performed independently for each subsystem, since the matrix takes the form

$$\begin{pmatrix} H_1 & 0 \\ 0 & H_2 \end{pmatrix}.$$

Since the Hilbert space is finite-dimensional, there will be L eigenvalues and L orthogonal eigenvectors that determine the full dynamics of the system. With the analogy with section 2 in mind, I start the system in an initial state $\psi_i = 1/\sqrt{L_s}$ for $i \in \{1, \cdots, L_s\}$ and $\psi_i = 0$ otherwise. Initially, then, the electron is confined to the left well. To create the plot analogous to Figure 2.2, but integrated over all possible energies, I evolve the wave function and plot the probability density summed only over the first L_s states (this is the analogy of the projector operator). For $t_1 = 0$, there should be no contact between the two chains, and so this value should be identically 1 for all time. For a small t_1, the leakage should be slow. I perform the calculation for a chain of $L = 30$ sites, with $L_s = 10$. First, I choose the hopping integral in each chain to be $t_0 = 1$ and the coupling between chains to be $t_1 = 0.005$. The results, illustrating the slow leakage, are shown below.

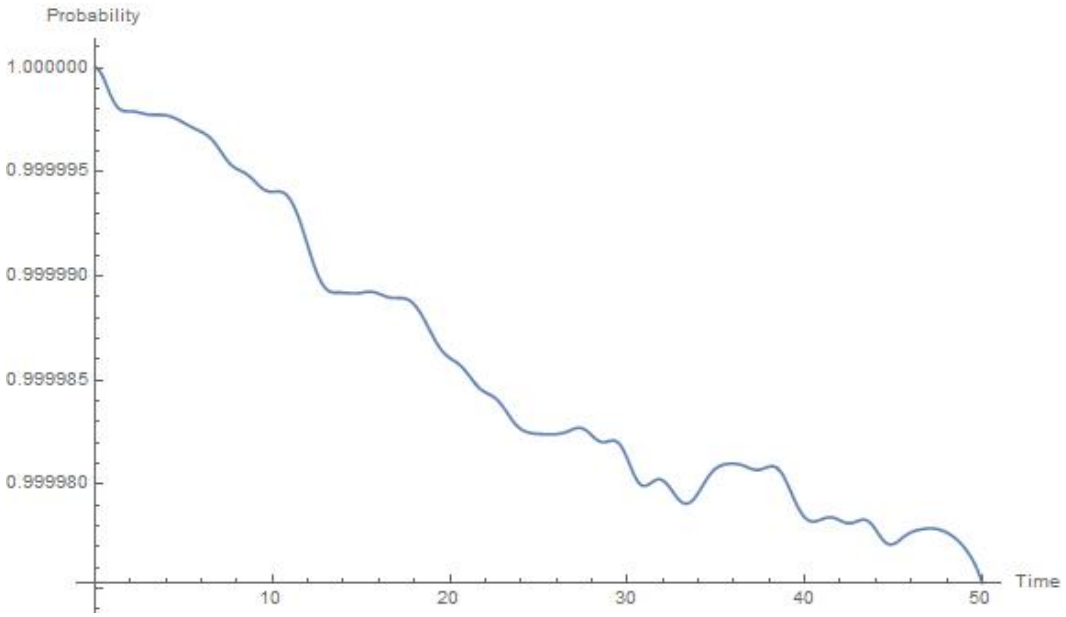

Figure 3.1: Slow leakage from one chain into another

The same parameters are kept for the following image, but with a stronger coupling between chains of $t_1 = 0.5$.

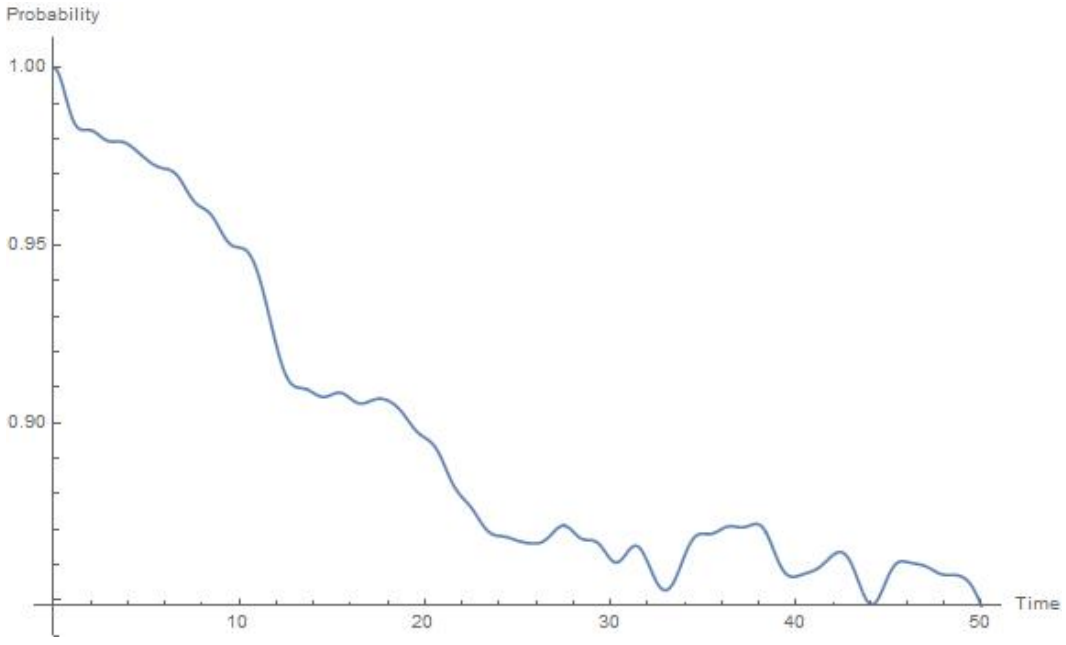

Figure 3.2: Fast leakage from one chain into another

As expected, the stronger coupling causes the initial leakage of the system to proceed much faster. Just as in the continuous system, plotting for longer times gives effects from the finite size of the well. Indeed, there seems to be a long-term oscillation effect where most of the probability density function for the electron travels *back* into the smaller left chain in finite time:

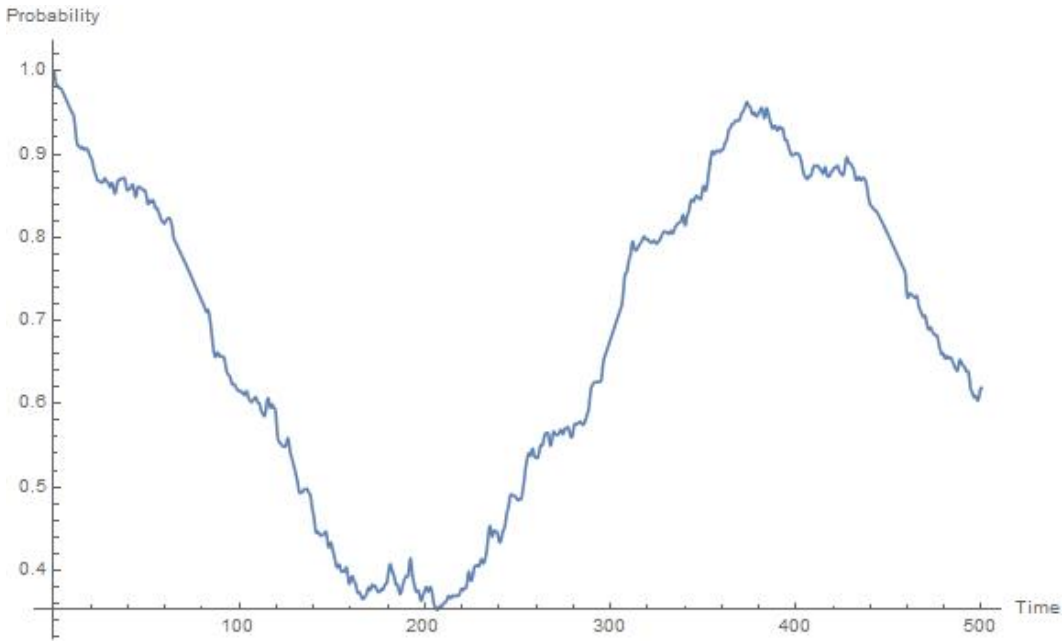

Figure 3.3: Long-term behavior of leakage in the discrete system

3.2 Code

Below is the (short!) Mathematica code used to generate the plots in this section.

```
size = 30;
Ls = 10;
t0 = -1;
t1 = -0.5;
eps = 0;
H0 = SparseArray[{{i_, i_} ->
     eps, {i_, j_} /;
      Abs[i - j] ==
        1 && {i, j} != {Ls, Ls + 1} && {i, j} != {Ls + 1, Ls} ->
     t0, {Ls, Ls + 1} -> t1, {Ls + 1, Ls} -> t1}, {size, size}, 0.0];
{energy, states} = Eigensystem[H0];
psi0 = Flatten[
   Append[ConstantArray[1/(Ls^(1/2)), Ls],
    ConstantArray[0, size - Ls]]];
psi[t_] :=
  Sum[psi0.states[[i]]*Exp[I*energy[[i]]*t]*states[[i]], {i, 1, size}];
Pdf[t_] := psi[t]*Conjugate[psi[t]];
P[t_] := Sum[Pdf[t][[i]], {i, 1, Ls}];
Plot[P[t], {t, 0, 500}, ImageSize -> Large,
 AxesLabel -> {"Time", "Probability"}]
```

Bibliography

[1] MIT Open Courseware. MIT Lecture: Reflection and Transmission at a Potential Step. *EECS Lecture Notes*, 2011.

[2] R.P. Feynman. Statistical Mechanics: A Set of Lectures. *Advanced Book Classics*, 1998.

Stephen J. Thornton

Education:

Pennsylvania State University Schreyer Honors College, University Park, PA May 2019

B.S. Physics, B.S. Mathematics, B.S. Astronomy & Astrophysics, M.A. Mathematics

Graduate Coursework: Measure Theory, Partial Differential Equations I, Partial Differential Equations II, Differentiable Manifolds, Fundamental Astrophysics, Stellar Structure, Functional Analysis, Homogenization Theory/Machine Learning, Math Grad Seminar

Research:

Theoretical Topological Mechanics REU, University of Pennsylvania, PA Summer 2018

- Worked with Prof. Bo Zhen to investigate the Su-Schrieffer-Heeger model for polyacetylene and determine an electrical circuit analogue supporting topologically protected states.

Theoretical Condensed Matter Physics Research, Penn State, PA August 2016 - Present

- Worked with Prof. Jorge Sofo to model the effects of disorder on different arrangements of atoms using quantum mechanics principles and Wolfram Mathematica.

Computational Astrophysics REU – Pulsars, Cornell University, NY Summer 2017

- Developed a code pipeline to detect statistically significant pulsars in VLA data.
- Presented a poster summarizing the results of this research at the 231st American Astronomical Society Meeting in January 2018.

Mathematical Magnetohydrodynamics Research, Penn State, PA February 2017 – Present

- Investigated astrophysical implications of flow solutions and modifications due to magnetization of the fluids as in the case of high-kT plasmas (magnetohydrodynamics).
- Determined consistency of local flow solutions with helical symmetry in MHD equations and geometric limits of such solutions using non-traditional disk projection methods.

Activities:

Learning Assistant – Astronomy of the Distant Universe, Penn State, PA Spring 2018

Focus for Teens 2017 – Outreach Event, Ithaca, NY Summer 2017

NRAO Community Day – Telescope Setup, Ithaca, NY Summer 2017

Awards:

- John & Elizabeth Holmes Teas Scholarship – Full Tuition 2018 – 2019
- Leonhard Euler Memorial Scholarship – Excellence in Mathematics March 2018
- Kadtke Scholarship – Excellence in Astrophysics March 2018
- McCubbin Fellowship – Excellence in Physics 2017 – 2018
- Sigma Pi Sigma Member – Physics Honor Society March 2018
- Eberly College of Science Diversity and Climate Award Nominee January 2018
- Dean's List, every semester 2015 – 2018
- Braddock Scholarship 2015 – 2019
- Schreyer Honors College Scholarship 2015 – 2019
- Eagle Scout Rank – Boy Scouts of America November 2015